Pharm Res (2010) 27:1900–1913
DOI 10.1007/s11095-010-0190-y

RESEARCH PAPER

Evaluation of Temperature-Sensitive, Indocyanine Green-Encapsulating Micelles for Noninvasive Near-Infrared Tumor Imaging

Tae Hee Kim • Yongping Chen • Christopher W. Mount • Wayne R. Gombotz • Xingde Li • Suzie H. Pun

Received: 9 April 2010 / Accepted: 4 June 2010 / Published online: 22 June 2010

ABSTRACT

Purpose Indocyanine green (ICG), an FDA-approved near infrared (NIR) dye, has potential application as a contrast agent for tumor detection. Because ICG binds strongly to plasma proteins and exhibits aqueous, photo, and thermal instability, its current applications are largely limited to monitoring blood flow. To address these issues, ICG was encapsulated and stabilized within polymeric micelles formed from the thermo-sensitive block copolymer Pluronic F-127, poly(ethylene oxide)-poly(propylene oxide)-poly(ethylene oxide), to increase the stability and circulation time of ICG.

Methods ICG-loaded Pluronic micelles were prepared at various concentrations of Pluronic and ICG and characterized by determining particle sizes, dye loading efficiency, and the kinetics of dye degradation. Förster resonance energy transfer spectroscopy was employed to monitor the stability of Pluronic micelles in physiological solutions. The plasma clearance kinetics and biodistribution of ICG-loaded micelles was also determined after intravenous delivery to CT-26 colon carcinoma tumor-bearing mice, and NIR whole-body imaging was performed for tumor detection.

Results The Pluronic F-127 micelles showed efficient ICG loading, small size, stabilized ICG fluorescence, and prolonged circulation *in vivo*. Solid tumors in mice were specifically visualized after intravenous administration of ICG-loaded micelles.

Conclusions These materials are therefore promising formulations for noninvasive NIR tumor imaging applications.

KEY WORDS indocyanine green · thermo-sensitivity · micelle · stability · near-infrared tumor imaging

INTRODUCTION

Near-infrared (NIR) fluorescence optical imaging has become an increasingly attractive technology for noninvasive disease diagnosis, treatment monitoring and drug screening (1). The NIR region (700–900 nm) is advantageous for sensitive *in vivo* optical imaging due to low autofluorescence background, low optical scattering and significant imaging depth (2–4). Indocyanine green (ICG) is a water-soluble and amphiphilic tricarbocyanine dye, belonging to the polymethine class of NIR contrast agents, and is the only NIR dye approved by the United States Food and Drug Administration (FDA) for medical diagnosis (5,6). Due to its low toxicity and capacity to absorb and emit in the NIR spectral range, it has been widely used for angiography and for evaluation of cardiac output and hepatic function (7–10). Recently, much attention has been focused on the potential use of ICG for early detection of shallow tumors such as breast cancer (11–13) and tumor destruction by photodynamic therapy based on its photosensitizing property (14,15). For both applications, it is

T. H. Kim • Y. Chen • C. W. Mount • X. Li • S. H. Pun (✉)
Department of Bioengineering, University of Washington
Box 355061, William H. Foege Building, 3720 15th Ave NE
Seattle, Washington 98195-5061, USA
e-mail: spun@u.washington.edu

W. R. Gombotz
Omeros Corporation
1420 Fifth Avenue, Suite 2600
Seattle, Washington 98101, USA

Present Address:
Y. Chen · X. Li (✉)
Department of Biomedical Engineering, Johns Hopkins University
720 Rutland Avenue Ross 731B
Baltimore, Maryland 21205, USA
e-mail: xingde@jhu.edu

crucial to achieve effective ICG delivery to the tumor site and accumulation and retention of ICG in the tumor (16). Additionally, pharmaceutically attractive formulations with good storage and shelf-life are important for clinical use.

The use of ICG for tumor imaging applications is limited by several ICG properties (6,13). The amphiphilic character of ICG induces aggregation in aqueous solution resulting in adverse effects on its optical properties, such as lower quantum yields due to self quenching (17,18). Also, tumor localization is limited to a rather short period of time after administration due to the strong plasma protein binding of ICG and subsequent rapid clearance by the liver (19). Furthermore, ICG undergoes degradation in aqueous media, resulting in a loss of absorption and fluorescence due to saturation of the double bonds in the conjugated chain (20). A potential approach to overcome these disadvantages is ICG delivery in nanoparticle systems that provide increased stability, protection from nonspecific plasma protein binding, and enhanced circulation time (21).

Polymeric nanoparticles are promising delivery vehicles for various cancer therapeutic and imaging applications (22). Nanoparticles can accumulate at tumors due to their leaky vasculature, ineffective lymphatic drainage, and enhanced endocytotic activity. This phenomenon is known as the enhanced permeation and retention (EPR) effect and provides a mechanism for passive targeting of nanoparticles to tumor sites (23). In addition, polymeric nanocarriers can be chemically modified and functionalized for site-specific targeting (24,25). Polymeric carriers such as poly(lactic-co-glycolic acid)(PLGA) nanoparticles (diameter ~360 nm) and silica-polymer composite microcapsule (diameter ~0.6 to 2 μm) containing ICG showed significantly increased photostability and plasma half-life compared to free ICG in solution (13,16,26). However, both of these ICG carriers lie in the upper limit of the preferred size range for imaging of metastatic cancer. Several recent publications have reported promising results with smaller nanoparticles. For example, Rodriguez *et al.* prepared poly (styrene-alt-maleic anhydride) block-poly(styrene) micelles (diameter ~55 nm) loaded with ICG and showed that the micelles stabilized ICG fluorescence with minimal cytotoxicity (21). The size of micelles, approximately 10–100 nm, is small enough to reduce clearance by the reticuloendothelial system (RES) and allow for enhanced EPR effect (27–30). Thus, incorporating ICG into micelles using a simple aqueous-based preparation method is an advantageous way to deliver ICG for early cancer detection (20).

In this study, we have employed Pluronic F-127 (PF-127, PEO_{100}-PPO_{65}-PEO_{100}) polymeric micelles for ICG delivery *in vivo*. PF-127 was selected because it is approved by the FDA for parenteral use (17,31). Additionally, the thermosensitive micellization property of PF-127 is another advantage for efficient ICG stabilization and tumor localization *in vivo* (32). There are several reports about the potential use of Pluronic block copolymers as a promising drug carrier for cancer therapy (33). However, for diagnostic NIR imaging applications, there is a lack of knowledge about the *in vitro* and *in vivo* stability of ICG dye encapsulated in Pluronic micelles.

Therefore, to investigate the potential use of micelles for NIR tumor imaging, ICG was loaded into Pluronic micelles at various concentrations of Pluronic and ICG and characterized by measuring micelle size distribution, dye loading efficiency, and both aqueous and thermal stability. Förster resonance energy transfer (FRET) spectroscopy was employed to monitor the release of dye and dissociation of Pluronic micelles in various aqueous solutions *in vitro*. To determine the circulation kinetics and biodistribution of ICG-loaded micelles *in vivo*, free ICG and ICG-loaded micelles were injected in the tail vein of CT-26 tumor-bearing mice, and the concentration of ICG in tumor, plasma and various organs was determined. Finally, a NIR *in vivo* imaging study was performed to observe the passive targeting of ICG-loaded micelles to solid tumor.

MATERIALS AND METHODS

Materials

Pluronic F-127 (PEO_{100}-PPO_{65}-PEO_{100}, Mw=12,600), indocyanine green (ICG), 3,3′-dioctadecyloxacarbocyanine perchlorate (DiO), and 1,1′-dioctadecyl-3,3,3′,3′-tetramethylindocarbocyanine perchlorate (DiI) were purchased from Sigma-Aldrich (St. Louis, MO, USA). Tetrabutylammonium iodide (TBAI) was obtained from Acros Organics (Morris Plains, NJ). Solvents used were ACS grade and obtained from J. T. Baker Chemical Co. (Phillipsburg, NJ) with the exception of chloroform (EMD, Gibbstown, NJ).

Preparation of ICG-Encapsulating PF-127 Micelle

A solvent evaporation method was employed to encapsulate ICG into the micelles after complexing ICG with TBAI to form a hydrophobic ICG-tetrabutylamine salt as previously described (21). Briefly, 1 mM ICG solution was prepared in chloroform with a six-fold molar excess of TBAI. After 30 min sonication, the ICG solution was then added dropwise to a stirring micelle solution in various concentrations of PF-127 (0, 2, 10, 20, 30, and 50 mg/mL) to achieve final ICG concentrations of 5, 10, and 20 μM. The chloroform was evaporated off to incorporate ICG into the hydrophobic cores of Pluronic micelles. Free ICG was removed using Amicon regenerated cellulose centrifuge filters (MWCO 10 kDa, Millipore, Billerica, MA), and the remaining ICG-loaded micelle solution was rinsed two

times using deionized (DI) water. Purified micelles were resuspended in the original volume of DI water, and lyophilized using a Labconco FreeZone 2.5 benchtop freeze dryer (Labconco, Kansas City, MO).

ICG Loading Efficiency and ICG Content

Lyophilized micelles were weighed and dissolved in 1 mL of dimethylformide (DMF), causing complete dissolution of the micelle and release of the encapsulated ICG. Empty micelles dissolved in DMF were used as a blank for ICG/micelle samples. The ICG concentration was determined by comparing absorbance at 775 nm to a standard curve of ICG with a squared correlation coefficient of 0.999 in the linear range of 0–12.5 μM in DMF. ICG content was expressed as the weight ratio between loaded ICG and total weight of ICG-loaded micelle, and loading efficiency as the weight percent of encapsulated ICG to total ICG initially used for encapsulation. All loading measurements were performed in triplicate.

Measurement of Micelle Sizes

The effective diameter of the PF-127 micelles prepared at various concentrations of Pluronic and ICG was measured using a ZetaPlus dynamic light scattering (DLS) instrument (Brookhaven Instrument Co., Holtsville, NY) at a wavelength of 659 nm with a 90-deg detection angle at both room temperature and 37°C. Each sample was analyzed in triplicate.

Aqueous and Thermal Stability of Studies

The stability of ICG encapsulated within PF-127 micelles was determined by assessing ICG fluorescence emission over a 10-day period. To compare the fluorescence intensity of free ICG prepared under the same conditions as micelle-encapsulated ICG, ICG solutions were prepared by adding ICG/TBAI complex into water, and chloroform was evaporated for the same time duration as ICG-loaded micelles were prepared. The ICG-loaded micelles were prepared in different aqueous solutions (water, phosphate-buffered saline (PBS) pH 7.4, 50% serum, 5% albumin, and 5% glucose) and then placed in a shaking incubator at either room temperature or 37°C. The micelle solutions were shaken horizontally at 100 rpm in the dark between readings. At predetermined time intervals, 100 μL of free ICG, unloaded micelle, and micelle-encapsulated ICG solutions were pipetted into a black 96-well plate with clear bottom, and fluorescence spectra of the ICG were measured from 786 to 850 nm (bandwidth 5 nm) using a Safire 2 microplate reader (Tecan, Austria) at an excitation of 775 nm (bandwidth 5 nm). For each reading, all settings such as the gain, integration time, number of reads, z-position of the scanner, and temperature were kept constant. The emission intensities of free ICG and ICG loaded within micelles were compared before and after addition of different physiological solutions. For analysis, the maximal ICG emission intensity for each sample at a given time was normalized by corresponding ICG emission at time zero. The average normalized emission intensity for each triplicate sample set was plotted as a function of time.

FRET Spectroscopy

FRET micelles formulated by loading DiI and DiO into PF-127 micelles were used to study the release of core-loaded molecules from micelles *in vitro* (34). FRET micelles were prepared by the solvent evaporation method as previously described for ICG-loaded micelles, except a stock solution for the FRET pair was prepared by dissolving 1 mg of DiI and 1 mg of DiO in 500 μL chloroform. The FRET pair solution was then added to a PF-127 micelle solution (40 mg/mL) to obtain a final composition of 0.15% DiO and 0.15% DiI by weight. For stability studies, micelles were diluted by adding the same volume of water, 2× PBS, fetal bovine serum (FBS), or 10% glucose to prepare 2% Pluronic micelles in various physiological solutions, and placed in a shaking incubator (rpm:100) at 37°C in the dark. At predetermined time intervals, fluorescence spectra ranging from 495 to 620 nm of FRET micelles were obtained on Tecan Safire 2 microplate reader with 484 nm excitation. The fluorescence spectra of lyophilized FRET micelles dissolved in DMSO were compared with those of FRET micelles in water.

Cell Lines and Cell Culture

CT-26 murine colon adenocarcinoma cells purchased from ATCC (Manassas, VA) were cultured in RPMI-1640 medium (Mediatech Inc, Manassas, VA) with 10% FBS and 1% antibiotic/antimicrobial at 37°C in 5% CO_2.

Animals and Tumor Implantation

Pathogen free Balb/c mice were housed in separate cages with normal access to food and water and kept on a 12-h light-dark cycle. All experimental procedures were performed in accordance with the protocols approved by the Institutional Animal Care and Use Committee at the University of Washington. To generate tumors, the back of 6-week-old female Balb/c mice was shaved and 100 μL of single cell suspension containing 2×10^6 CT-26 cells in serum-free RPMI-1640 was injected subcutaneously under

anesthesia. After 7~10 days, mice were injected with ICG or ICG-loaded micelles. Mice were anesthetized using an intraperitoneal (i.p.) injection of a ketamine/xylazine mixture (130 mg/kg ketamine and 8.8 mg/kg xylazine).

In Vivo Study—Circulation Kinetics and Biodistribution

ICG and ICG-loaded micelle solutions (150 μL) were injected intravenously (i.v.) through the tail vein of CT-26 tumor-bearing mice at a dose of 10 μg ICG. A second injection was performed with the same dose of ICG and ICG-loaded micelles. Blood was collected at various time points, and all the mice were sacrificed at the last time point to harvest various major tissues including liver, lung, heart, kidney, spleen, and tumor. A fluorescence-based assay was used to analyze ICG in the biological samples as previously described (16). Briefly, the blood samples were diluted by adding 100 μL of DMSO, and ICG was extracted for 10 min. Tissue samples were homogenized with 1 mL of DMSO, followed by overnight extraction at room temperature in the dark. The mixtures of blood and tissues were then centrifuged at 10,000 rpm for 10 min and the supernatant containing the extracted ICG was measured by fluorescence spectroscopy. The fluorescence intensity of ICG in plasma was normalized by protein content as measured by BCA Protein Assay Kit (Pierce, Rockford, IL). The amount of ICG in tissue was calculated according to a standard curve with a squared correlation coefficient of 0.993 in the linear range of 0–0.25 μg/mL and normalized by weight of tissue. The tissue and plasma samples from the non-treated animals were analyzed to determine the background fluorescence.

In Vivo NIR Fluorescence Imaging

In vivo optical imaging was performed with a Xenogen IVIS® Spectrum imaging system (Caliper Life Science, Hopkinton, MA, USA) with an ICG filter set (excitation: 745 nm; emission: 800 nm). Mice were injected with ICG and ICG-loaded PF-127 micelles via double tail vein at total dose of 20 μg ICG. After sacrifice, the tumors and major organs were isolated and imaged again. For quantitative comparison, regions of interests (ROIs) were drawn over tumors, and the total fluorescence efficiency ([p/s/cm^2/sr]/[μW/cm^2]; photons per second per centimeter squared per steradian per microwatt per centimeter squared) was measured.

Data Analysis

Data are expressed as mean ± standard deviation, and statistical analysis was performed using unpaired Student's *t*-test. Data were considered significantly different at $P<0.05$.

RESULTS

Characterization of ICG Encapsulating-PF-127 Micelles

ICG was converted to the hydrophobic tetrabutylammonium salt and encapsulated into the hydrophobic PF-127 micelle core by solvent evaporation. The loading efficiency of ICG was calculated by determining the fraction of ICG content in the micelles compared to the amount of ICG used during micelle formulation. As summarized in Table I, the efficiency of ICG loading ranged from 39–78% and was dependent on the concentration of ICG and PF-127 during formulation. Efficiency of ICG loading within micelles was increased with increasing concentrations of ICG and decreasing concentrations of PF-127. The average diameter of ICG-loaded micelles was determined to be 20–30 nm at 37°C by dynamic light scattering (Table I). Encapsulation of ICG does not significantly affect micelle size for PF-127 concentrations above 2%. ICG concentration during formulation does not affect micelle size within the concentrations tested (5 μM to 20 μM).

The absorbance and fluorescence spectra of free ICG were compared to the spectra of micelle-encapsulated ICG prepared in various concentrations of PF-127 at 37°C. As shown in Fig. 1, red-shifts were observed in both the absorbance and emission spectra of encapsulated ICG (9 nm and 13 nm, respectively), indicating ICG entrapment within micelle. A significant decrease in fluorescence emission of 10 μM free ICG was observed because ICG is known to self-quench at the concentrations above 5 μM in aqueous solutions (35). Additionally, the ICG/TBAI hydrophobic salt is even more prone to self-aggregation in water. The fluorescence intensity of encapsulated ICG increased with increasing concentrations of PF-127 despite decreases in ICG loading efficiency. The encapsulated ICG is likely uniformly distributed in the Pluronic micelles based on the elevated fluorescence intensity of encapsulated ICG, and ICG encapsulation is highly efficient when the concentration of Pluronic is above 1%.

Aqueous Stability and Thermal Stability of Encapsulated ICG

The poor stability of ICG dye in aqueous solution is undesirable in its development for clinical applications as a NIR contrast agent. To determine whether encapsulation of ICG dye in PF-127 micelles protects ICG from degradation, the aqueous stability of ICG in various concentrations of PF-127 was investigated at both room temperature and 37°C. The fluorescence intensity of free ICG and ICG encapsulated within various concentrations of PF-127 was monitored in water for 10 days and normalized by the initial fluorescence

Table I Characteristics of the ICG-Loaded PF-127 Micelles

ICG/Pluronic F-127 micelle	Feed concentration of ICG (μM)	Loading efficiency (%) [a]	ICG content (μg/mg) [b]	Micelle diameter (nm) [c]	PDI [d]
2% PF-127	0	–	–	22.5 ± 0.8	0.068
5 μM ICG/2% PF-127	5	51.6 ± 0.7	0.1 ± 0.001	22.9 ± 0.9	0.051
10 μM ICG/0.2% PF-127	10	n.d.	n.d.	27.1 ± 1.2	0.130
10 μM ICG/1% PF-127	10	77.9 ± 1.9	0.6 ± 0.01	28.9 ± 1.1	0.177
10 μM ICG/2% PF-127	10	72.4 ± 3.5	0.28 ± 0.01	22.6 ± 0.7	0.067
10 μM ICG/3% PF-127	10	61.4 ± 2.8	0.16 ± 0.01	21.8 ± 1.1	0.067
10 μM ICG/5% PF-127	10	38.6 ± 3.1	0.06 ± 0.005	19.9 ± 0.9	0.104
20 μM ICG/2% PF-127	20	78.5 ± 0.6	0.6 ± 0.005	22.1 ± 0.5	0.087

[a] Weight percent of experimental ICG loading to total ICG feed ($n = 3$)

[b] Weight ratio between encapsulated ICG and total weight of ICG-loaded micelle

[c] Effective diameter measured by dynamic light scattering at 37°C with 5 runs per measurements

[d] Polydispersity index measured by dynamic light scattering at 37°C

n.d.= not determined

intensity of each sample. The fluorescence emission of free ICG decreased rapidly over time at room temperature (Fig. 2a), and the kinetics of fluorescence loss were even faster for solutions stirred at physiological temperature (Fig. 2b), indicating severe degradation of ICG. However, the fluorescence emission of micelle-encapsulated ICG showed a much slower decrease with time compared to that of free ICG at both temperatures. The ICG micelle solutions showed higher stability at 37°C compared to room temperature. ICG stability was also improved when formulated with higher concentrations of PF-127 micelles; however, there was no significant difference in ICG stability when the concentration of ICG used in the formulations is changed (data not shown). These results demonstrate that the key parameter for controlling ICG stability in micelles is the concentration of PF-127 copolymer used in formulations.

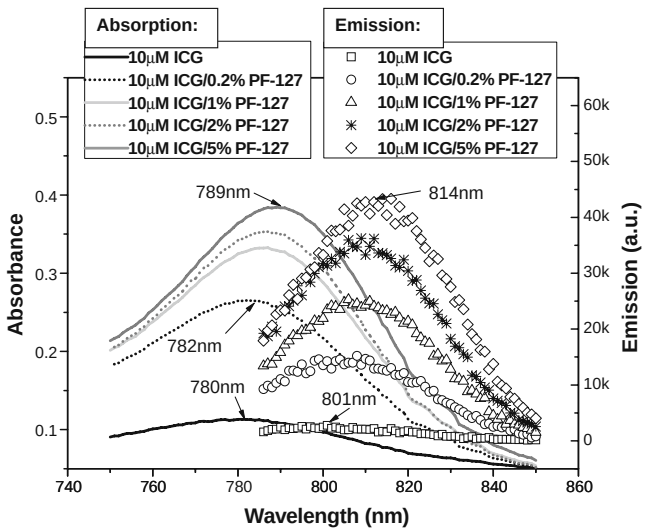

Fig. 1 Absorbance and emission spectra of free ICG and ICG-loaded PF-127 micelle prepared with various concentrations of PF-127 and measured at 37°C.

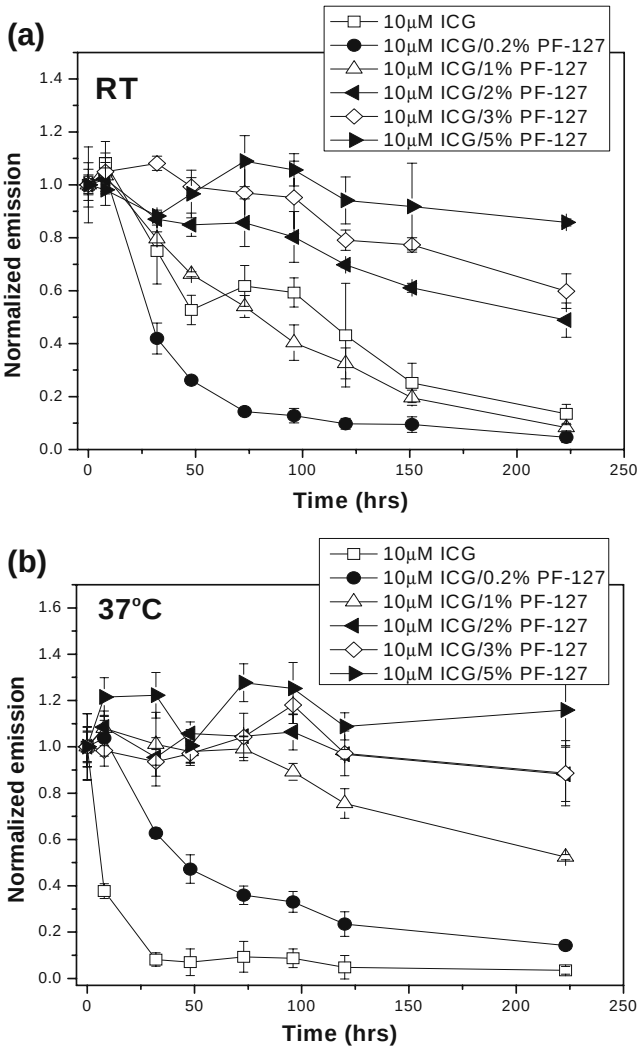

Fig. 2 Relative fluorescence emission of free ICG and ICG encapsulated in various concentrations of PF-127 micelles over 10 days incubated at (**a**) room temperature and (**b**) 37°C ($n = 3$).

It is important to note that the ICG-TBAI salt shows only 20% of fluorescence intensity when compared to freshly prepared ICG solution because a significant loss of fluorescence from free ICG occurs even during preparation due to rapid decomposition (36). Due to this lower initial fluorescence of free ICG, the decrease of fluorescence seems to be slower than some ICG-loaded micelles at room temperature. However, the absolute intensity value was much less than that of ICG-loaded micelles (data not shown). We also compared the stability of the ICG/TBAI complex with ICG solution prepared by just dissolving water-soluble ICG in water. The decrease of fluorescence intensity of ICG solution was much faster than that of ICG/TBAI complex at body temperature (data not shown), indicating that ICG/TBAI complex can be rapidly aggregated in aqueous solution, but degradation of ICG can be retarded within hydrophobic salt form.

The fluorescence emission of ICG remained nearly constant over 10 days at physiological temperature when the concentration of PF-127 was higher than 2% (Fig. 2b). Even after 3 weeks, 5% Pluronic micelles still maintained the same fluorescent emission value as freshly prepared ICG-loaded micelles (data not shown). The effect of temperature on ICG stability can be clearly observed by comparing the fluorescence of encapsulated ICG in 1% PF-127 micelles at both temperatures over 10 days. The fluorescence emission of free ICG solution decreased by 90% at room temperature, whereas micelle-encapsulated ICG was significantly protected from thermal degradation, maintaining 90% of original emission for 96 h and showing only 48% decrease over 10 days of incubation at 37°C. This indicates higher ICG stability in polymeric micelles at physiological temperatures due to the temperature-dependent micellization property of Pluronic itself.

For *in vivo* imaging applications, the stability of ICG was investigated in more physiologically relevant solutions. First, the emission intensities of free ICG and ICG encapsulated within 2% PF-127 micelles were compared before and after addition of either 5% glucose (injection media), PBS, or FBS. The emission intensities in these solutions were normalized by the emission intensity of ICG in water at the time of analysis. The fluorescence intensity of free ICG was drastically decreased in PBS solution (60% lower than in water) and significantly increased by 280% with addition of FBS (Fig. 3a). However, encapsulated ICG in micelles exhibited no significant change after addition of the various solutions, indicating the excellent protection of ICG from contact with the environmental conditions. As shown in Fig. 3b, the fluorescence intensity of free ICG in PBS and 5% glucose solution decreased rapidly over time, whereas that of encapsulated ICG remained constant in all three different solutions for more than 3 weeks. Since free ICG can

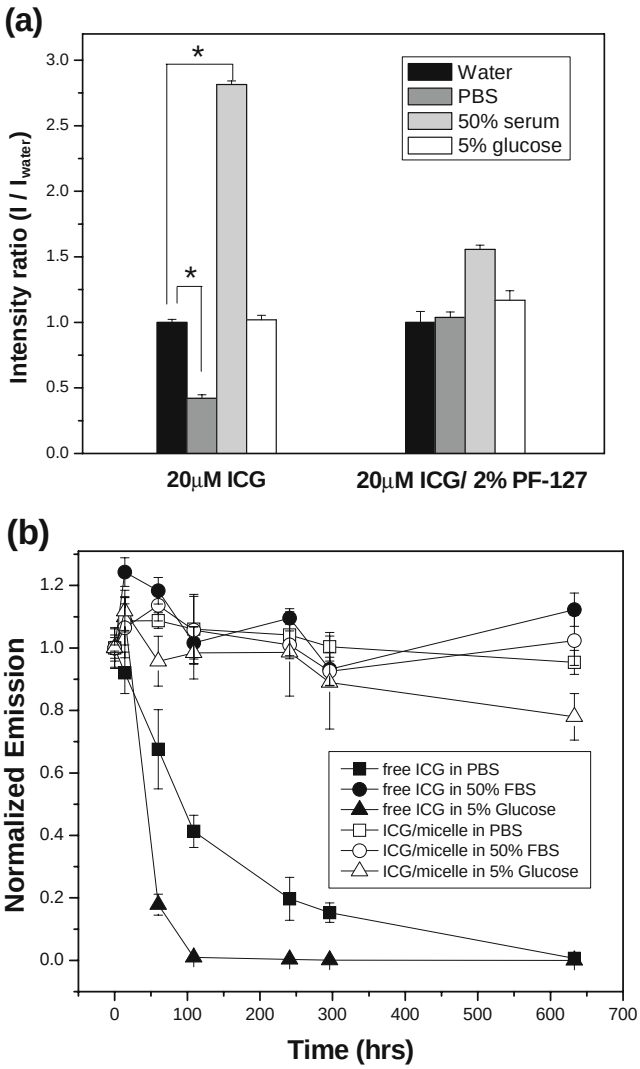

Fig. 3 Stability study of free ICG and ICG loaded in PF-127 micelles in various physiological solutions. (**a**) Emission intensity of free ICG and ICG loaded in 2% PF-127 micelles in various solutions normalized by that in water (* indicates a statistically significant difference from fluorescence intensity measured in water using the student's *t*-test, $p < 0.05$, $n = 3$) (**b**) Relative fluorescence emission of 20 μM ICG and 20 μM ICG encapsulated in 2% PF127 micelles in various physiological media over 3 weeks ($n = 3$).

easily bind to proteins, resulting in dye stabilization and nearly constant fluorescence with time, it was not possible to compare the stability between free ICG and encapsulated ICG in serum. Therefore, fluorescence resonance energy transfer (FRET) spectroscopy was employed to monitor the release of core-loaded dyes from Pluronic micelle in various physiological solutions *in vitro*.

The FRET pair DiO (a green fluorescent lipophilic probe as a donor) and DiI (a red-orange fluorescent lipophilic probe as an acceptor) was loaded into 2% PF-127 micelles, and the occurrence of FRET was confirmed by fluorescence spectra of FRET micelles in water or DMSO measured with 484 nm excitation. Efficient FRET

was observed from micelles in water due to the close proximity of DiO and DiI in the micelle core with highest fluorescence intensity at 585 nm. After micelle disruption by DMSO, FRET disappeared due to the release of dyes increasing distance between FRET pair and resulting in only DiO signal at 502 nm (Fig. 4a).

The stability of FRET micelles was then evaluated in various physiological solutions. As shown in Fig. 4b–e, minimal DiO and DiI release was observed up to a 2-h incubation period in all the different solutions. Efficient FRET, an indication of intact micelles, was observed even after 12 hrs of incubation in water or 5% glucose solution as shown in Fig. 4b and e. Micelles were slightly less stable after 12 h incubation in PBS solution (Fig. 4c). A significant increase of DiO fluorescence intensity was obtained after 12 h incubation in FBS solution, indicating the instability of micelles and faster release of dyes from the micelle core with prolonged incubation in serum (Fig. 4d). However, micelles showed good stability within 2 h incubation in FBS solution, implying possible maintenance of micelle stability in blood serum during the 50 min biodistribution study performed in this study.

In Vivo Biodistribution Study

The biodistribution of ICG in tumor-bearing mice was investigated after ICG or ICG-loaded PF-127 micelles were administered to the tail vein. To achieve prolonged plasma circulation, a second dose was injected 30 min after the first dose. Fig. 5a shows ICG fluorescence intensity within the blood at various post-injection times. When ICG was delivered via Pluronic micelles, the ICG concentration in the blood was higher (3.8-fold higher at 5 min) than when given as free ICG solution. The residence time of ICG-micelles within plasma was also enhanced; nevertheless, the ICG fluorescence intensity is rapidly decreased by 20 min. After the second injection, the fluorescence intensity of ICG-micelle in plasma was highly increased. In addition, the residence time of ICG in plasma is notably increased for up to 2 hr with ICG-micelle-treated mice compared to free-ICG-treated mice.

The biodistribution of ICG was determined after the two injections. One-and-a-half hours after the second injection, tumors and major organs were excised and ICG was isolated by DMSO extraction. As shown in Fig. 5b, the majority of ICG accumulated within the liver, with lower amounts of ICG recovered from the heart, lung, spleen, and kidney. Although not statistically significant, a trend of increased ICG levels in the most of major organs for ICG-loaded Pluronic micelle system was obtained when compared to free ICG solution. A significantly higher ICG accumulation was observed in the tumor when ICG was delivered via micelle system. Representative NIR fluorescence images of dissected organs and tumors are shown in Fig. 5c. Higher fluorescence signals were observed in tumor, kidney, lung, and liver when ICG was delivered by PF-127 micelles. In Fig. 6, tumors collected from all mice (4 mice in each group) were imaged, and ICG fluorescence intensity was quantitatively compared between two groups by image analysis. Tumors from mice treated with ICG-loaded PF-127 micelles showed significantly higher ICG fluorescence efficiency than tumors from mice treated with free ICG. These results correlate with values obtained by ICG extraction (Fig. 5b) and indicate that (i) PF-127 micelles can accumulate in tumors by passive EPR targeting and (ii) NIR imaging is a reliable alternative method to ICG extraction for evaluating the ICG content in tissues.

Whole-Body NIR Imaging

Mice treated with free ICG and ICG-loaded PF-127 micelles were imaged at 36 h and 5 day post-injection with representative images shown in Fig. 7a. When the mice were imaged at 2 h post-injection, it was difficult to get clear images due to the strong ICG signal from the liver and the background signals due to ICG circulating in the blood. After 36 h, ICG was mostly cleared by the liver, and the target tumor was specifically visualized with ICG-loaded micelles, whereas mice injected with free ICG solution showed very weak ICG signal in tumor. The same mice were imaged again at 5 d post-injection. There was negligible decrease of ICG fluorescence efficiency in tumor (~9%), as compared to 36 h post-injection image. From the dissected organs, a high fluorescence signal in tumor was observed 5 day after administration of ICG-loaded PF-127 micelles (Fig. 7b). These results suggest that PF-127 micelle can be an efficient ICG delivery system for tumor targeting, and also for potential tumor diagnosis for long-term follow-up.

DISCUSSION

In this work, ICG was successfully encapsulated and stabilized within thermosensitive PF-127 micelles. At room temperature, both the hydrophilic EO and hydrophobic PO blocks within a Pluronic molecule are hydrated and are relatively soluble in water, but when temperature is above the critical micelle temperature, the PO block dehydrates and becomes insoluble, resulting in the formation of compact micelles of 20–30 nm size (37). Higher concentrations of PF-127 resulted in smaller micelle diameters with lower loading efficiency, possibly due to less space available for ICG molecules in the smaller micelles (Table I). At concentrations equal to or greater than 2% PF-127, micelles with good stability are formed. At 2% and 3% PF-127, unimodal distributions of micelles with average diameters ~20–25 nm are formed. At 5% PF-127, a

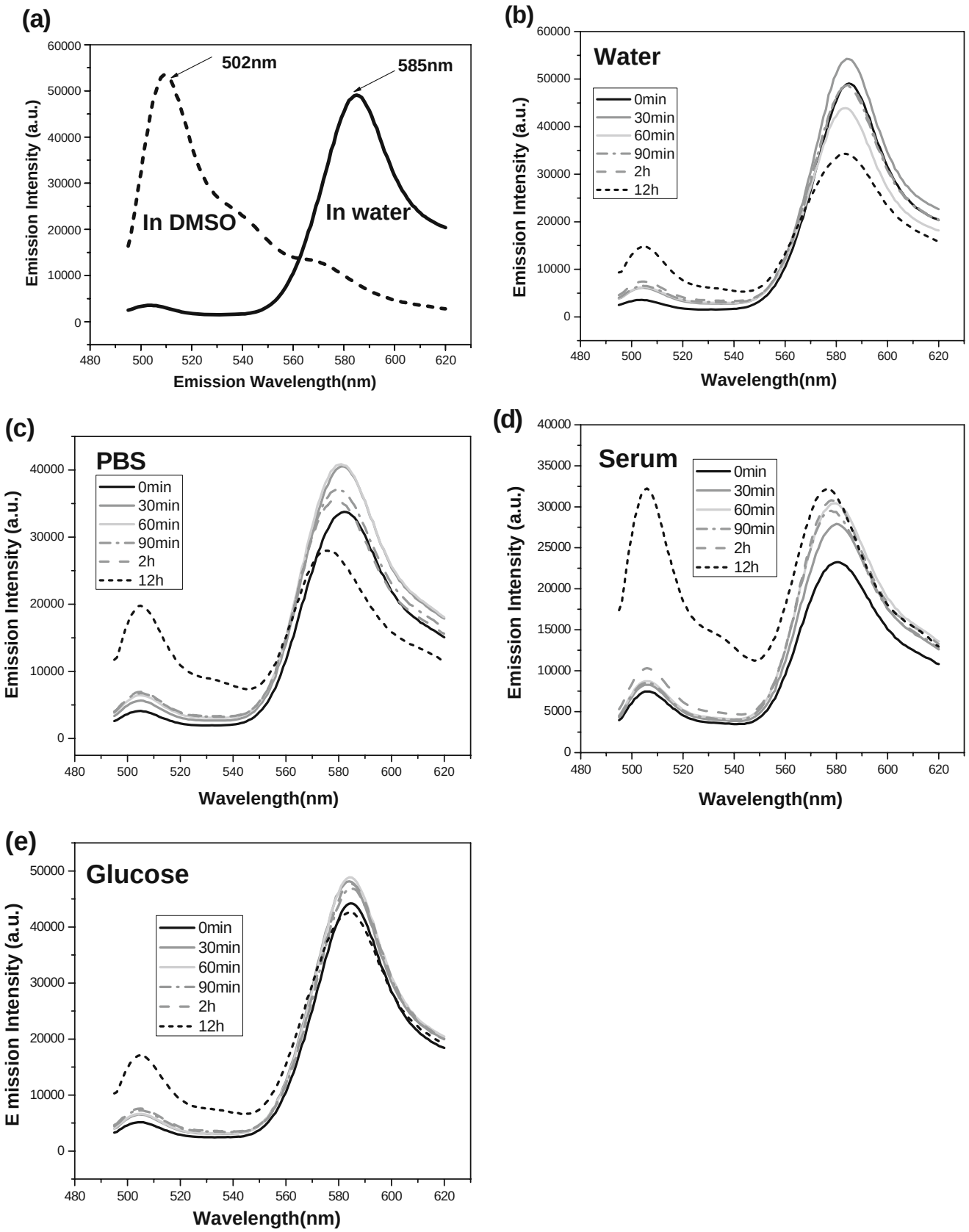

Fig. 4 Fluorescence spectral measurement of FRET micelle measured in various solutions. (**a**) water (solid line) and DMSO (dashed line) (**b**) water (**c**) PBS (**d**) 50% serum and (**e**) 5% glucose incubated at 37°C over 12 h.

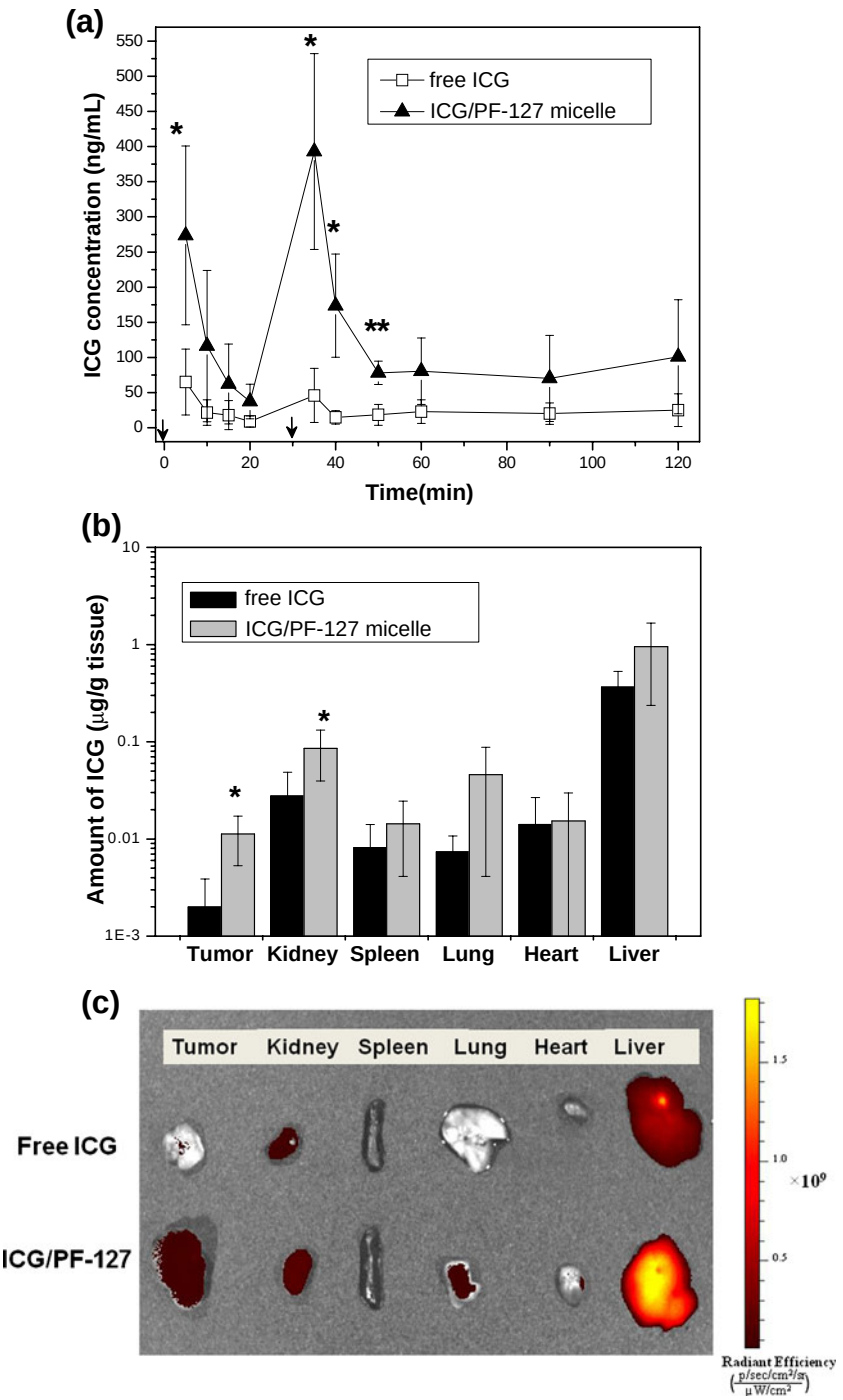

Fig. 5 *In vivo* biodistribution of free ICG and ICG loaded in PF-127 micelles after CT-26 tumor-bearing mice after double i.v. injections (1st dose: 10 μg ICG, 2nd dose: 10 μg ICG, 30 min after the 1st injection). (**a**) Time course of *in vivo* fluorescence intensity of ICG in mouse blood serum at various time course (arrows represent time points of the first and second injections) (**b**) Quantification of ICG in various organs at 1.5 hr after second injection (* and ** indicate a statistically significant difference from free ICG using the student's *t*-test, $p < 0.05$ and $p < 0.01$, respectively, $n = 4$) (**c**) Representative fluorescence image of dissected organs from mice sacrificed at 2 hr post-injection. Colors indicate the relative fluorescence.

bimodal distribution is observed. This is also reflected by the larger polydispersity index. The primary population has average diameter ~13 nm. Accordingly, ICG loading efficiency is significantly lower for this formulation. Larger micelles with higher aggregation number have been found to be more efficient at solubilizing drugs due to their sufficiently larger and more hydrophobic core (38).

ICG encapsulation was confirmed by a red-shift in the absorbance and fluorescence maxima of ICG-encapsulating Pluronic micelles (Fig. 1). The red-shifts have been previously reported in other ICG-loaded micellar systems such as Pluronic F-68,Solutol HS 15 and ICG-loaded PLGA nanoparticles (13,20,21,39). Saxena *et al.* noted a significant decrease of fluorescence emission intensity due to self-quenching between the closely packed ICG molecules in PLGA nanoparticles (13). However, in our study, the fluorescence intensity of ICG encapsulated within PF-127 was much higher than that of free ICG and increased with increasing concentrations of PF-127. This enhanced brightness may be attributed to more uniform distribution, less self-

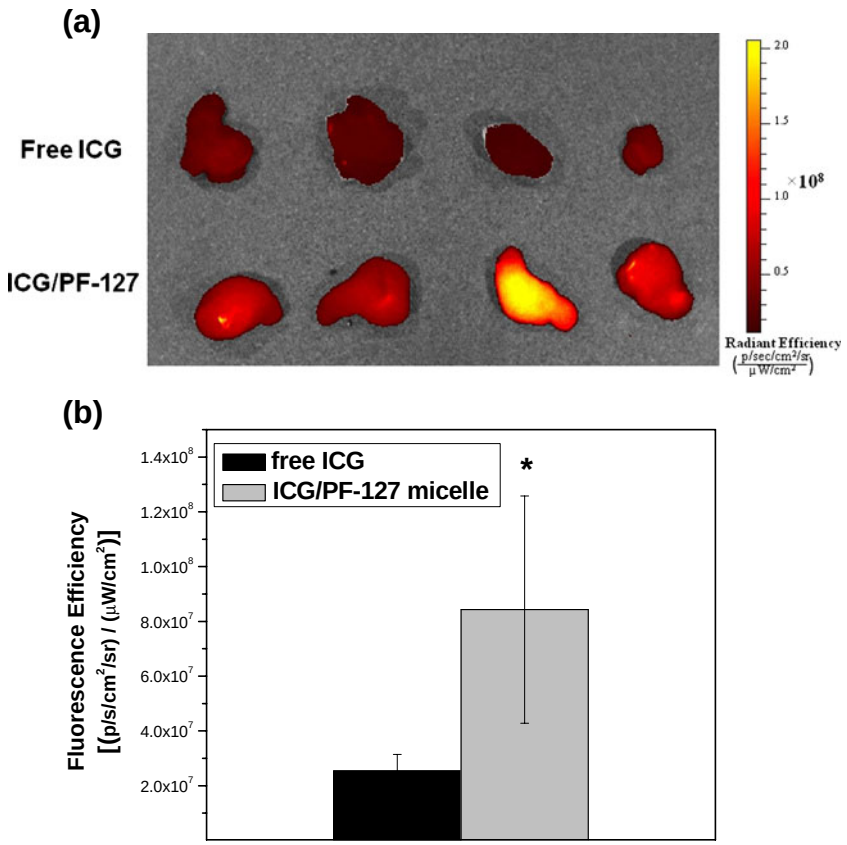

Fig. 6 Detection of ICG fluorescence in tumor tissues dissected from CT-26 tumor-bearing mice at 2 hr after double i.v. injections with free ICG and ICG-loaded PF-127 micelle (**a**) NIR fluorescence imaging of dissected tumors (**b**) Measurement of fluorescence efficiency using Living Image® software and a ROI tool for imaging analysis (* indicates a statistically significant difference from free ICG using the student's *t*-test, $p < 0.05$, $n = 4$).

aggregation, and less self-quenching of ICG with higher numbers of micelles. As reported from a previous study, the enhanced fluorescence with a red-shift of the emission peak can be observed when ICG is embedded at the interface between hydrophobic core and hydrophilic shell of micelles (40). Amphiphilic ICG incorporating into the interface of the surfactant micellar structures of PF-127 can lead to the partitioning of ICG with reduction of aggregation. Several systems have reported an increase in the aqueous stability of ICG over 3–5 days after incorporation into nanoparticulate systems (13,21,26). Rodriguez *et al.* obtained aqueous stability of ICG-loaded micelles over 2 weeks at room temperature, but at body temperature, 63% loss in ICG emission intensity was observed after 2 weeks (21). However, the thermosensitive PF-127 micelles showed excellent ICG stabilizing ability at body temperature (Figs. 2 and 3).

Decreases in ICG fluorescence intensity during the incubation are likely related to several factors, including micelle dissociation, release of ICG from the micelles, and the ICG degradation. After incubation of micelles for 3 weeks at 37°C, significant decreases in micelle size were observed for concentrations of 0.2% and 1% PF-127; in contrast, no significant change in micelle size was observed for concentrations of 2%, 3% and 5% PF-127. The decrease of diameter of micelles can indicate ICG release. This data indicates that less ICG is released at concentrations of PF-127 ≥ 2%, resulting in stabilization of ICG emission intensity.

Because micelle stability and albumin binding both result in stabilization of ICG fluorescence, it was not clear if ICG fluorescence in ICG-loaded micelles incubated in serum is preserved because of protection of ICG by the micelles or due to the release of ICG from micelles and subsequent binding to serum proteins. Recently, a FRET imaging method was applied to reveal the release of hydrophobic molecules *in vitro* and *in vivo* from poly(ethylene glycol)-poly(D,L-lactic acid) micelles (PEG-PDLLA) (41,42). For a better understanding of ICG stabilization within Pluronic micelles, the same lipophilic FRET pair was entrapped into Pluronic micelle cores (Fig. 4). Pluronic micelles loaded with DiO alone or DiI alone excited at 484 nm showed minimal cross-talk and direct acceptor excitation in comparison with FRET pair within the micelle core (data not shown). Minimal FRET dye release was observed in both water and 5% glucose solution for 12 hrs (Fig. 4). These results support the stability of ICG-micelles shown by fluorescence measurements in Fig. 3. A slight reduction in FRET efficiency was observed for micelles in PBS, despite no decrease in ICG fluorescence from comparable formulations. One possible explanation is that ICG may experience a quenching effect in the core of micelle. It should be noted that ICG at 20 μM is known to

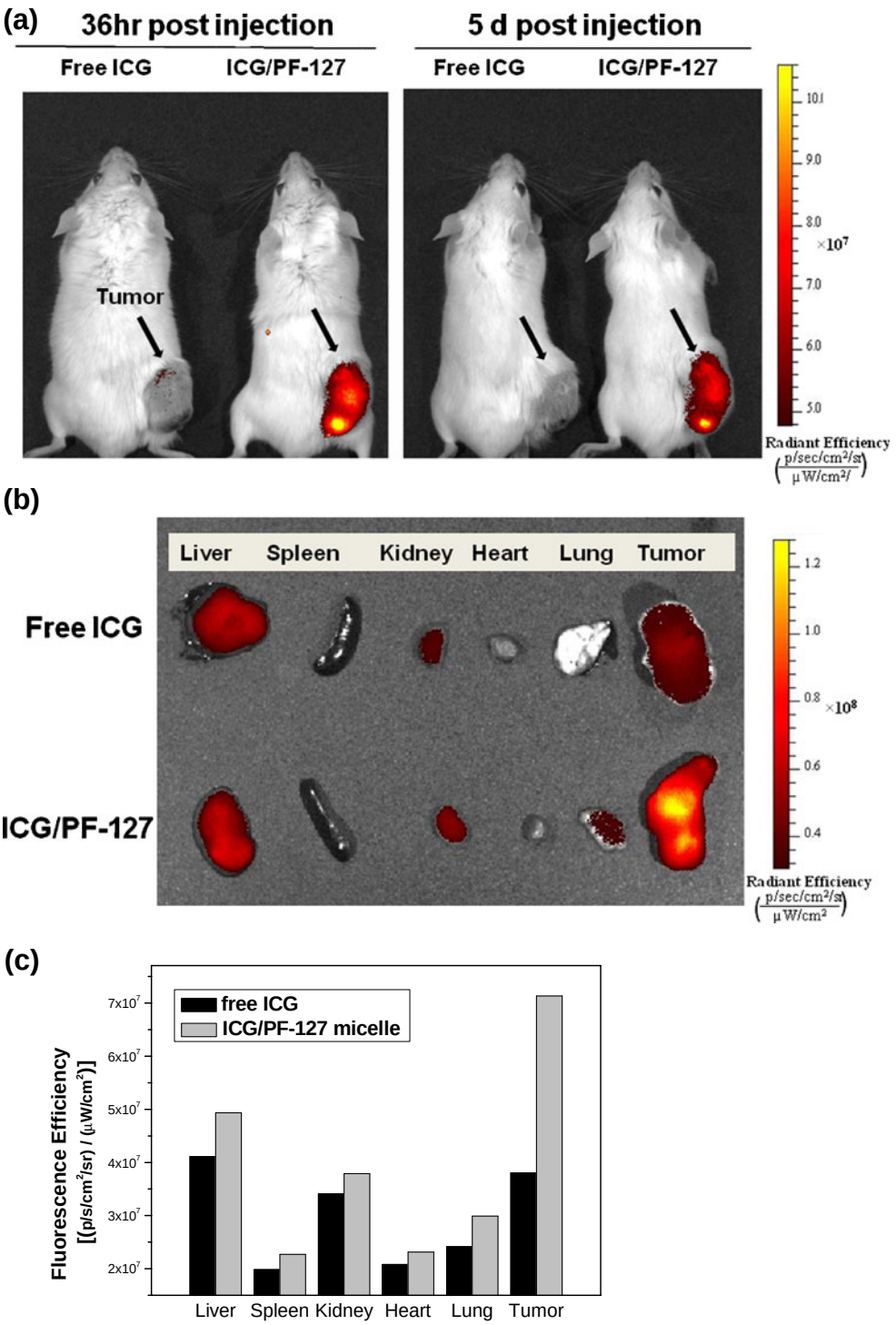

Fig. 7 *In vivo* tumor imaging. (**a**) Representative whole-body NIR images of CT-26 tumor-bearing mice at 36 hrs and 5 days after injection of free ICG and ICG-loaded PF-127 micelle. (black arrows: tumor) (**b**) Representative fluorescence image of dissected organs from mice sacrificed at 5 day post-injection. (**c**) Measurement of fluorescence efficiency using Living Image® software and a ROI tool for imaging analysis.

have self-quenching in aqueous solution (35). If ICG is partially self-quenched in the core of micelles, the fluorescence intensity of ICG can remain relatively constant even when ICG is partially released from the micelles due to a reduction in dye quenching within the micelle. The observation that no fluorescence change occurred in ICG-loaded micelles despite a 25% decrease in absorbance by 9 days (data not shown) supports this hypothesis. In a recent study, the major factor for the fast disassembly of PEG-PDLLA (poly(ethylene glycol)-poly(D,L-lactic acid) micelles *in vivo* was found to be in blood plasma (34). However, Pluronic micelles were observed to be more stable than PEG-PDLLA micelles because no significant change in FRET signals was observed in 2 h incubation in serum. The kinetics of ICG release from PF-127 micelles may therefore be advantageous for tumor imaging applications if micelles

can deliver ICG to the tumor site within 2 h. ICG-loaded PF-127 micelles are stable for long periods in storage conditions at 37°C but will gradually destabilize and release their contents over the course of several hours in the presence of serum.

Passive targeting via the EPR effect relies on tumor accumulation that results from selective extravasation at the tumor site and prolonged circulation (25). ICG binds to albumin and α-lipoprotein in blood plasma, leading to rapid clearance from blood (plasma $t_{1/2}$=2–4 min) (13,39,43). In our study, higher ICG fluorescence intensity in plasma was initially observed at 5 min after administration of ICG-encapsulating micelles such that initial micelle concentration in blood was >200-fold higher than the critical micelle concentration (CMC, 2.8×10^{-6}M) (44). However, by 20 min post-injection, both free ICG and ICG-loaded micelles were mostly cleared from the blood (Fig. 5). A second dose of ICG-loaded PF-127 micelles administered 30 min after the first dose significantly enhanced ICG circulation time in blood. This effect can be attributed to both increased micelle concentration in the blood and a decrease in phagocytic clearance of micelles by the RES due to saturation of these cells from the initial dose. Recently, le Masne de Chermont *et al.* reported that i.v. tail vein preinjection of anionic liposomes to mice presaturated RES uptake capacity and significantly improved the circulation time of the PEGylated inorganic luminescent nanoparticles injected 5 min after preinjection and thus the potential for specific targeting (45). A similar effect of double injection on RES saturation was also observed in our study, resulting in enhancement of blood circulation time and tumor accumulation. In addition, the PEG outer shell of PF-127 micelles can sterically hinder interactions with proteins, leading to higher stability and longer circulation time (46). Recently, the accelerated blood clearance (ABC) phenomenon for removal of PEGylated nanoparticles due to anti-PEG IgM secretion from splenic B cells was reported (47,48). One of the important factors for ABC phenomenon is size, and the ABC was not observed with 9.7–31.5 nm polymeric micelles (49). Due to thermosensitive property of PF-127, ICG-loaded micelles show uniform and compact size in 20–30 nm at 37°C. In addition, with such a short time interval for secondary dose, ABC is unlikely to occur for this system.

At 2 hrs post-injection, the highest fluorescence signal for both ICG- and ICG-micelle-treated mice was in the liver (Fig. 6). This is not surprising, because ICG is reported to be consumed by hepatic parenchymal cells lining the liver's sinusoids, which then eliminates ICG from the bloodstream unmetabolized through biliary excretion (43,50,51). Nanoparticles such as micelles are also primarily cleared from the body by resident macrophages in the liver. Although there are several reports on the *in vivo* biodistribution of Pluronic micelles, the published reports specifically on the biodistribution of PF-127 after intravenous injection are sparse. Pluronic P85 was reported to have high accumulation in liver, kidney and spleen, decreasing in the following order: liver > spleen > kidney > lungs > brain (46). We observed a similar trend showing slightly higher fluorescence of ICG-loaded micelles than free ICG in those organs.

The utility of micellar carriers for therapeutic applications is highly correlated to their *in vivo* stability. In this study, we used live animal optical imaging to demonstrate that PF-127, with its excellent biocompatibility profile, can be administered at sufficient concentration to be used for tumor-targeted delivery in a mouse xenograft model (Figs. 6 and 7). Tumor localization of ICG was strongly enhanced after ICG was encapsulated within PF-127 micelles, consistent with the results of longer circulation of micelles in blood (Fig. 5). In addition, due to the thermosensitive property of PF-127, CMC is much lower at body temperature than room temperature (25°C: 0.555 mM; 35°C: 0.019 mM) (52), resulting in the formation of uniform micelles of 20–30 nm size. This feature can be very useful as a noninvasive method for monitoring tumor response to chemotherapy or applying to photodynamic therapy.

In summary, Pluronic micelles are a promising vehicle for ICG delivery for noninvasive tumor imaging due to their ideal size with narrow size distribution, excellent stabilizing ability at physiological temperature, and prolonged circulation time. Moreover, the surface of the micelles can potentially be engineered for specific purposes such as incorporation of a targeting ligand for active tumor targeting. This study is the first report to demonstrate that PF-127 micelle shows excellent tumor accumulation via EPR effect for efficient NIR tumor imaging. Clinical translation may also be facilitated because both components, PF-127 and ICG, are already FDA approved.

CONCLUSIONS

The present study demonstrated that encapsulation of ICG within polymeric micelles formed from thermosensitive PF-127 triblock copolymer showed simple aqueous-based preparation, efficient ICG loading, small size, stabilized ICG fluorescence over varied conditions and long time periods, and prolonged circulation time *in vivo*. Our results suggest the great potential of the PF-127 micelle system to improve noninvasive ICG imaging for cancer detection and assessment of therapeutic interventions by allowing long-term stability of ICG *in vitro* and tumor-targeting *in vivo*.

ACKNOWLEDGEMENTS

This work was supported by the funds from the Washington Technology Center and Omeros Corporation (Pun and Li),

and in part by the National Institutes of Health (Grant No. R01 CA120480-Li). Xenogen Spectrum imaging was conducted through the Center for Intracellular Delivery of Biologics, funded by Washington State Life Sciences Discovery Fund Grant 2496490.

REFERENCES

1. Ke S, Wen X, Gurfinkel M, Charnsangavej C, Wallace S, Sevick-Muraca EM, *et al.* Near-infrared optical imaging of epidermal growth factor receptor in breast cancer xenografts. Cancer Res. 2003;63:7870–5.
2. Klohs J, Wunder A, Licha K. Near-infrared fluorescent probes for imaging vascular pathophysiology. Basic Res Cardiol. 2008;103:144–51.
3. Taroni P, Pifferi A, Torricelli A, Comelli D, Cubeddu R. *In vivo* absorption and scattering spectroscopy of biological tissues. Photochem Photobiol Sci. 2003;2:124–9.
4. Licha K, Olbrich C. Optical imaging in drug discovery and diagnostic applications. Adv Drug Deliv Rev. 2005;57:1087–108.
5. Rao J, Dragulescu-Andrasi A, Yao H. Fluorescence imaging *in vivo*: recent advances. Curr Opin Biotechnol. 2007;18:17–25.
6. Saxena V, Sadoqi M, Shao J. Degradation kinetics of indocyanine green in aqueous solution. J Pharm Sci. 2003;92:2090–7.
7. Slakter JS, Yannuzzi LA, Guyer DR, Sorenson JA, Orlock DA. Indocyanine-green angiography. Curr Opin Ophthalmol. 1995;6:25–32.
8. Caesar J, Shaldon S, Chiandussi L, Guevara L, Sherlock S. The use of indocyanine green in the measurement of hepatic blood flow and as a test of hepatic function. Clin Sci. 1961;21:43–57.
9. Maarek JM, Holschneider DP, Rubinstein EH. Fluorescence dilution technique for measurement of cardiac output and circulating blood volume in healthy human subjects. Anesthesiology. 2007;106:491–8.
10. Paumgart G, Probst P, Kraines R, Leevy CM. Kinetics of indocyanine green removal from blood. Ann N Y Acad Sci. 1970;170:134–47.
11. Intes X, Ripoll J, Chen Y, Nioka S, Yodh AG, Chance B. *In vivo* continuous-wave optical breast imaging enhanced with Indocyanine Green. Med Phys. 2003;30:1039–47.
12. Ntziachristos V, Yodh AG, Schnall M, Chance B. Concurrent MRI and diffuse optical tomography of breast after indocyanine green enhancement. Proc Natl Acad Sci U S A. 2000;97:2767–72.
13. Saxena V, Sadoqi M, Shao J. Enhanced photo-stability, thermal-stability and aqueous-stability of indocyanine green in polymeric nanoparticulate systems. J Photochem Photobiol B. 2004;74:29–38.
14. Fickweiler S, Szeimies RM, Baumler W, Steinbach P, Karrer S, Goetz AE, *et al.* Indocyanine green: intracellular uptake and phototherapeutic effects *in vitro*. J Photochem Photobiol B. 1997;38:178–83.
15. Kim G, Huang SW, Day KC, O'Donnell M, Agayan RR, Day MA, *et al.* Indocyanine-green-embedded PEBBLEs as a contrast agent for photoacoustic imaging. J Biomed Opt. 2007;12:044020.
16. Saxena V, Sadoqi M, Shao J. Polymeric nanoparticulate delivery system for Indocyanine green: biodistribution in healthy mice. Int J Pharm. 2006;308:200–4.
17. Choi SH, Lee JH, Choi SM, Park TG. Thermally reversible pluronic/heparin nanocapsules exhibiting 1000-fold volume transition. Langmuir. 2006;22:1758–62.
18. Cardillo JA, Jorge R, Costa RA, Nunes SM, Lavinsky D, Kuppermann BD, *et al.* Experimental selective choriocapillaris photothrombosis using a modified indocyanine green formulation. Br J Ophthalmol. 2008;92:276–80.
19. Licha K, Riefke B, Ntziachristos V, Becker A, Chance B, Semmler W. Hydrophilic cyanine dyes as contrast agents for near-infrared tumor imaging: synthesis, photophysical properties and spectroscopic *in vivo* characterization. Photochem Photobiol. 2000;72:392–8.
20. Kirchherr AK, Briel A, Mader K. Stabilization of indocyanine green by encapsulation within micellar systems. Mol Pharm. 2009;6:480–91.
21. Rodriguez VB, Henry SM, Hoffman AS, Stayton PS, Li X, Pun SH. Encapsulation and stabilization of indocyanine green within poly(styrene-alt-maleic anhydride) block-poly(styrene) micelles for near-infrared imaging. J Biomed Opt. 2008;13:014025.
22. Soppimath KS, Aminabhavi TM, Kulkarni AR, Rudzinski WE. Biodegradable polymeric nanoparticles as drug delivery devices. J Control Release. 2001;70:1–20.
23. Peer D, Karp JM, Hong S, Farokhzad OC, Margalit R, Langer R. Nanocarriers as an emerging platform for cancer therapy. Nat Nanotechnol. 2007;2:751–60.
24. Blanco E, Kessinger CW, Sumer BD, Gao J. Multifunctional micellar nanomedicine for cancer therapy. Exp Biol Med (Maywood). 2009;234:123–31.
25. Romberg B, Hennink WE, Storm G. Sheddable coatings for long-circulating nanoparticles. Pharm Res. 2008;25:55–71.
26. Yu J, Yaseen MA, Anvari B, Wong MS. Synthesis of near-infrared-absorbing nanoparticle-assembled capsules. Chem Mater. 2007;19:1277–84.
27. Liu H, Farrell S, Uhrich K. Drug release characteristics of unimolecular polymeric micelles. J Control Release. 2000;68:167–74.
28. Moghimi SM, Porter CJ, Muir IS, Illum L, Davis SS. Non-phagocytic uptake of intravenously injected microspheres in rat spleen: influence of particle size and hydrophilic coating. Biochem Biophys Res Commun. 1991;177:861–6.
29. Yuan F, Dellian M, Fukumura D, Leunig M, Berk DA, Torchilin VP, *et al.* Vascular permeability in a human tumor xenograft: molecular size dependence and cutoff size. Cancer Res. 1995;55:3752–6.
30. Stolnik S, Illum L, Davis SS. Long circulating microparticulate drug carriers. Adv Drug Deliv Rev. 1995;16:195–214.
31. Bhardwajand R, Blanchard J. Controlled-release delivery system for the alpha-MSH analog melanotan-I using poloxamer 407. J Pharm Sci. 1996;85:915–9.
32. Bae KH, Lee Y, Park TG. Oil-encapsulating PEO-PPO-PEO/PEG shell cross-linked nanocapsules for target-specific delivery of paclitaxel. Biomacromolecules. 2007;8:650–6.
33. Batrakova EV, Kabanov AV. Pluronic block copolymers: evolution of drug delivery concept from inert nanocarriers to biological response modifiers. J Control Release. 2008;130:98–106.
34. Chen H, Kim S, He W, Wang H, Low PS, Park K, *et al.* Fast release of lipophilic agents from circulating PEG-PDLLA micelles revealed by *in vivo* forster resonance energy transfer imaging. Langmuir. 2008;24:5213–7.
35. Rajagopalan R, Uetrecht P, Bugaj JE, Achilefu SA, Dorshow RB. Stabilization of the optical tracer agent indocyanine green using noncovalent interactions. Photochem Photobiol. 2000;71:347–50.
36. Sauda K, Imasaka T, Ishibashi N. Determination of protein in human-serum by high-performance liquid-chromatography with semiconductor-laser fluorometric detection. Anal Chem. 1986;58:2649–53.
37. Kabanov AV, Batrakova EV, Alakhov VY. Pluronic block copolymers as novel polymer therapeutics for drug and gene delivery. J Control Release. 2002;82:189–212.
38. Malmsten M, Lindman B. Self-assembly in aqueous block copolymer solutions. Macromolecules. 1992;25:5440–5.
39. Gomes AJ, Lunardi LO, Marchetti JM, Lunardi CN, Tedesco AC. Indocyanine green nanoparticles useful for photomedicine. Photomed Laser Surg. 2006;24:514–21.

40. Devoisselle JM, Soulie-Begu S, Mordon S, Desmettre T, Maillols H. Fluorescence properties of indocyanine green: I.*in-vitro* study with micelles and liposomes. In: Thompson RB, editor. *SPIE*, Vol. 2980, Advances in Fluorescence Sensing Technology III, San Jose, CA, USA; 1997, p. 530–537.
41. Altinoglu EI, Russin TJ, Kaiser JM, Barth BM, Eklund PC, Kester M, *et al*. Near-infrared emitting fluorophore-doped calcium phosphate nanoparticles for *in vivo* imaging of human breast cancer. ACS Nano. 2008;2:2075–84.
42. Chen H, Kim S, Li L, Wang S, Park K, Cheng JX. Release of hydrophobic molecules from polymer micelles into cell membranes revealed by Forster resonance energy transfer imaging. Proc Natl Acad Sci U S A. 2008;105:6596–601.
43. Yaseen MA, Yu J, Jung BS, Wong MS, Anvari B. Biodistribution of encapsulated indocyanine green in healthy mice. Mol Pharm. 2009;6:1321–32.
44. Kozlov MY, Melik-Nubarov NS, Batrakova EV, Kabanov AV. Relationship between pluronic block copolymer structure, critical micellization concentration and partitioning coefficients of low molecular mass solutes. Macromolecules. 2000;33:3305–13.
45. le Masne Q, de Chermont C, Chaneac JS, Pelle F, Maitrejean S, Jolivet JP, *et al*. Nanoprobes with near-infrared persistent luminescence for *in vivo* imaging. Proc Natl Acad Sci U S A. 2007;104:9266–71.
46. Batrakova EV, Li S, Li YL, Alakhov VY, Elmquist WF, Kabanov AV. Distribution kinetics of a micelle-forming block copolymer Pluronic P85. J Control Release. 2004;100:389–97.
47. Ishida T, Atobe K, Wang X, Kiwada H. Accelerated blood clearance of PEGylated liposomes upon repeated injections: effect of doxorubicin-encapsulation and high-dose first injection. J Control Release. 2006;115:251–8.
48. Ishida T, Ichihara M, Wang X, Yamamoto K, Kimura J, Majima E, *et al*. Injection of PEGylated liposomes in rats elicits PEG-specific IgM, which is responsible for rapid elimination of a second dose of PEGylated liposomes. J Control Release. 2006;112:15–25.
49. Koide H, Asai T, Hatanaka K, Urakami T, Ishii T, Kenjo E, *et al*. Particle size-dependent triggering of accelerated blood clearance phenomenon. Int J Pharm. 2008;362:197–200.
50. Tanaka E, Choi HS, Humblet V, Ohnishi S, Laurence RG, Frangioni JV. Real-time intraoperative assessment of the extrahepatic bile ducts in rats and pigs using invisible near-infrared fluorescent light. Surgery. 2008;144:39–48.
51. Desmettre T, Devoisselle JM, Mordon S. Fluorescence properties and metabolic features of indocyanine green (ICG) as related to angiography. Surv Ophthalmol. 2000;45:15–27.
52. Alexandridis P, Holzwarth JF, Hatton TA. Micellization of Poly (Ethylene Oxide)-Poly(Propylene Oxide)-Poly(Ethylene Oxide) Triblock Copolymers in Aqueous-Solutions—Thermodynamics of Copolymer Association. Macromolecules. 1994;27:2414–25.